

Biosensors for Detection of Organophosphate Exposure by New Diethyl Thiophosphate-Specific Aptamer

Napachanok Mongkoldhumrongkul Swainson

Kasetsart University - Bangkok Campus: Kasetsart University

Chonnikarn Saikaew

Kasetsart University - Bangkok Campus: Kasetsart University

Kanyanat Theeraraksakul

Kasetsart University - Bangkok Campus: Kasetsart University

Pongsakorn Aiemderm

Kasetsart University - Bangkok Campus: Kasetsart University

Rimduisit Pakjira

Department of Disease Control

Charoenkwan Kraiya

Chula: Chulalongkorn University

Sasimanas Unajak

Kasetsart University - Bangkok Campus: Kasetsart University

kiattawee choowongkomon (✉ fsciktc@ku.ac.th)

Kasetsart University <https://orcid.org/0000-0002-2421-7859>

Research Article

Keywords: Aptasensor, organophosphate metabolites, diethyl thiophosphate, electrochemical impedance spectroscopy, capillary electrophoresis

Posted Date: February 23rd, 2021

DOI: <https://doi.org/10.21203/rs.3.rs-217995/v1>

License: © ⓘ This work is licensed under a Creative Commons Attribution 4.0 International License.

[Read Full License](#)

Version of Record: A version of this preprint was published at Biotechnology Letters on July 6th, 2021. See the published version at <https://doi.org/10.1007/s10529-021-03158-2>.

Abstract

Objective An aptamer specifically binding to diethyl thiophosphate (DETP) was constructed and incorporated in an optical sensor and electrochemical impedance spectroscopy (EIS) to enable the specific measurement of DETP as a metabolite and a biomarker of exposure to organophosphates.

Results DETP-bound aptamer was selected from the library using capillary electrophoresis-systematic evolution of ligands by exponential enrichment (CE-SELEX). A colorimetric method revealed the aptamer had the highest affinity to DETP with a mean K_d value (\pm SD) of $0.103 \pm 0.014 \mu\text{M}$. Changes in resistance using EIS showed selectivity of the aptamer for DETP higher than for dithiophosphate (DEDTP) and diethyl phosphate (DEP) which have similar structure and are metabolites of some of the same organophosphates. The mean (\pm SD) of percentage of altered resistance of DETP was calculated at $47.5 \pm 8.8\%$ which was significantly higher than of DEDTP at $14.3 \pm 1.5\%$ and of DEP at $7.0 \pm 1.4\%$.

Conclusions The current method showed a great promise in using the DETP-specific aptamer to detect the exposure history to organophosphates, by measuring their metabolite, although degradation of organophosphate parent compounds might occur.

1. Introduction

Organophosphates are typically used as pesticides. Their contamination in the environment may result in their availability in agricultural products, water, soil and air. The metabolism of organophosphates in human beings, environmental matrices and microbes has generated dialkyl phosphates (Ohshiro et al. 1996; Racke 1992; Simaremare et al. 2019)

The metabolites of organophosphates comprise dimethyl phosphate (DMP), dimethyl thiophosphate (DMTP), dimethyl dithiophosphate (DMDTP), diethyl phosphate (DEP), diethyl thiophosphate (DETP) and diethyl dithiophosphate (DEDTP). Each corresponds to the exposure of one or more types of organophosphates. For example, DEP and DETP are metabolites of chlorethoxyphos, chlorpyrifos, coumaphos, diazinon, parathion and sulfotep. Additionally, DEP, DETP and DEDTP can be generated by the metabolism of disulfoton, ethion, phorate and terbufos (Sudakin and Stone 2011).

A study demonstrated that dialkyl phosphates were commonly found in fruits and vegetables although the levels of organophosphates were less than legal minimum levels (Zhang et al. 2008). DEP and DETP were found in purchased apples and oranges including the extracted juices that had been in cool storage for 3 days (Lu et al. 2005). Generally, dialkyl phosphates had greater persistence than their organophosphate parent compounds. Thus, it is difficult to measure trace amounts of organophosphates following progressive degradation in cold storage or as a result of biodegradation.

Traditional methods to detect dialkyl phosphates as a biomarker of exposure include gas chromatography (GC) and mass spectrometry due to their sensitivity and reliability (Kongtip et al. 2017).

However, chromatographic techniques require extensive sample pre-treatment, specialist operation and expensive equipment. Thus, these techniques are not suitable for screening dialkyl phosphates on-site.

This research aimed to overcome the false-negative detection of degraded organophosphates and enable detection of DETP, as a biomarker of exposure of organophosphates, using aptamer-based biosensor techniques. The DETP recognition unit was generated using CE-SELEX and selected the highest-affinity aptamer for DETP using a colorimetric method. The aptasensor was further fabricated using EIS to facilitate the selective measurement of DETP over any other metabolites which have similar structures to DETP.

2. Material And Methods

2.1 DNA aptamer selection for DETP

The selection of the aptamer from the random single-strand DNA (ssDNA) library was performed using the CE-SELEX method. The ssDNA of the library was composed of 40 variable bases in the middle and primer binding sites flanking the 5' and 3' ends. The capillary column was pre-rinsed with 50 mM 2-Morpholinoethanesulfonic acid (MES) buffer pH 7.4 for 10 minutes before pre-heated ssDNA library, 1 M of DETP or the mixture of the library and DETP was injected into the capillary for 30 seconds with 20 kV applied (Beckman Coulter). The detection was set at the separation voltage of 30 kV and incorporated with the absorbance at 254 nm (Varian). Sample fractions were collected during 2–4 minutes and used as a template for polymerase chain reaction (PCR) in the next step.

2.2 DETP-bound ssDNA enrichment and asymmetric PCR

DETP-bound ssDNA was amplified using a PCR technique. A sample (2 μ L) of the template from the previous step was mixed with buffer, 2mM dNTP, 5 μ M of forward and reverse primers and 1.0 U Taq DNA in 50 μ L final volume. The reaction started with 95°C for 5 minutes, followed by 30 cycles of 95°C for 30 seconds, 55°C for 30 seconds and 72°C for 10 seconds and finally at 72°C for 10 minutes.

To amplify forward and reverse strands of 0036, 0040, 0041, 0043, 0047 and 0048, asymmetric PCR was performed as previously mentioned, except that the ratio of the forward to reverse primer was 29:1 when forward strands were generated and 1:29 for reverse strand expansion.

2.3 Colorimetric screening for ssDNA candidates

The optimum amount (250 ng in 5 μ L) of each PCR and asymmetric PCR product was heated at 95°C for 10 minutes and then immediately put on ice for 5 minutes. They were then mixed with 37 μ L of gold nano-particle (AuNPs) and 5 μ L of targets or water (control) before adding 2.5 μ L of 2 N NaCl. Each step was performed at room temperature for 10 minutes of incubation. The absorbance at 520 nm and 650 nm was measured and compared with the controls. Three aptamer candidates tagged with thiol (-SH) group were then generated by the TianGen Company for further assessment of binding affinity.

2.4 Specificity and sensitivity assays by colorimetric method

Three selected aptamers at 0.5 μM was prepared to evaluate their ability to bind DETP and other metabolites as well as pesticides (DEDTP, DEP, DMP, paraquat and carbamate), for cross-selectivity. The sensitivity of the aptamers to DETP was measured using DETP at final concentrations of 0, 0.001, 0.005, 0.01, 0.05, 0.1, 0.5, 1, 2.5, 5, 10, 25, 50 and 100 μM as the target. The colorimetric method was performed as described previously.

2.5 Secondary structure of DETP-bound aptamers

The secondary structure of selected aptamers was analyzed using the RNAfold software (<http://rna.tbi.univie.ac.at/cgi-bin/RNAWebSuite/RNAfold.cgi>). DETP-binding sequences and structure were predicted.

2.6 Electrochemical measurements

Both the cyclic voltammetry (CV) and EIS experiments were carried out on a commercial screen-printed electrode (Metrohm) with a gold working electrode (4 mm diameter), using ferri/ferrocyanide ($\text{Fe}(\text{CN})_6^{3-/4-}$ in 0.1 M KCl) as the electrolyte. The measurements were conducted using a PalmSens4 potentiostat and the results were transferred and analyzed using the PSTrace software. CV scans were performed with a scanning range from -0.6 V to 0.8 V at a scanning rate of 10 mV/s and used to validate every electrochemical reaction occurring on the aptasensors. EIS was acquired at 5 mV amplitude within the frequency range of 0.1 Hz to 100 KHz.

A bare gold SPE was incubated with 5 μM of thiol-modified 0036F aptamer (0036F-SH) in phosphate buffer saline (PBS) at room temperature for 3 hours, washed with Milli-Q water and subsequently incubated with 1 mM of 6-mercapto-1-hexanol (MCH) for 10 minutes in order to block non-specific binding on the gold surface. The MCH/aptamer-Au electrode was washed with Milli-Q water and then measured charge transfer resistance (R_{ct}) before being used as an aptasensor to determine targets consisting 0.025 $\mu\text{g}/\text{ml}$ of DETP, DEDTP or DEP in PBS. They were incubated on the SPE for 10 minutes at room temperature, rinsed with Milli-Q water and subjected to electrochemical measurements. The impedance spectra were presented as Nyquist plots ($-Z''/\Omega$ versus Z'/Ω) with a sampling rate of 12 points per decade. The R_{ct} was recorded using the RCRW equivalent circuit.

3. Results And Discussion

3.1 Aptamer selection

The *in vitro* selection of DETP-specific aptamers from the library was carried out using CE-SELEX to overcome the drawbacks of conventional SELEX by eliminating stationary support, linker bias and kinetic bias (Mendonsa and Bowser 2004). Initially, ssDNA or pure DETP were analyzed for their mobility rate in

CE and eluted at 6-7.5 minutes (Fig. 1a) or 2.7 minutes (Fig. 1b), respectively. Afterward, electrophoresis was performed under the same conditions with a mixture of DNA library with DETP. The results are shown in Fig. 1c and revealed two separated fractions, eluted at 2.7 and 6.7 minutes, respectively. The eluted fraction at 2.7 minutes had two peaks with different intensities. This indicated that the formation of the complex with pure DETP shifted the migration rate of the aptamer-target complex to be closer to the migration rate of the target alone. This could have been due to conformational change after random ssDNA interacted with DETP which is a very small molecule. Therefore, DETP-bound ssDNA could have been separated from the ssDNA library by CE-SELEX and the eluent from 2 to 4 minutes was collected to enrich the targeted ssDNA aptamer in the next step.

The DETP-bound ssDNA was then amplified using a PCR technique. The PCR products were then cloned. Fifty colonies with expected sizes of PCR products (data not shown) were cultured before their plasmid was extracted and sequenced. The nucleotide sequences of the 50 recombinant plasmids revealed only 39 clones with the insertion of a 40 bp variable region and specific primer sequences. Thus, the PCR products from the 39 clones were further investigated for their affinity to DETP using the gold nanoparticle (AuNPs) colorimetric method.

3.2 Colorimetric screening for aptamer candidates

In principle, the ssDNA or denatured PCR products on the surface of the AuNPs prevent aggregation of the AuNPs after salt induction. Thus, the ssDNA-coated AuNPs maintain a red-wine color with λ_{\max} at 520 nm. The interaction between ssDNA and the target subsequently allows clumping of the AuNPs to occur in the presence of a monovalent positive charge (Na^+) and the color alters to purple with λ_{\max} at 650 nm instead.

The denatured PCR products of the 39 clones were assessed for their ability to detect the presence of DETP and thus allow the aggregation of the AuNPs after NaCl induction. A reduction in the absorbance at 520 nm of the aggregated particles was observed (Fig. 2a) and compared with the reaction where gold aggregation was not interfered by ssDNA (containing only AuNP, DETP and NaCl). The PCR products from clones 0036, 0040, 0041, 0043, 0047 and 0048 (grey bars in Fig. 2a) exhibited red-wine gold particle remnants to a similar extent as the control. Clones 0003, 0039 and 0042 also showed promising interaction to DETP; however, their controls (250 ng of ssDNA mixed with AuNPs and NaCl) also change to purple without DETP added (data not shown). This explained why the increased absorbance at 650nm was not investigated in this experiment, and only the remaining red-color particle should be of interest. Thus, the reduction of remaining ability to absorb light at 520 nm could inversely reflect the reaction rate for AuNPs aggregation, after conformational change by DETP-ssDNA interaction.

Selected ssDNA, forward (F) and reverse (R), was subsequently amplified using asymmetric PCR with the double strand PCR product from clones 0036, 0040, 0041, 0043, 0047 and 0048 as the template. Twelve aptamers were successfully generated and investigated the DETP-ssDNA interaction. The increase in the $A_{650}/A_{520\text{nm}}$ ratio upon target interaction was compared with the positive control comprising AuNPs and NaCl and the negative control without aggregation induction by NaCl. The results

(Fig. 2b) revealed 4 ssDNA strands with the highest absorbance ratio: OO36F, OO40F, OO40R and OO47F. In an asymmetric PCR reaction, non-targeted strands or the product of the lower concentration primer is also generated. Therefore, OO40F was selected due to its higher A₆₅₀/520nm ratio than OO40R, which was generated from the same template/PCR product. Then, OO36F, OO40F and OO47F were commercially synthesized with thiol group tagging at the 5' end and further assessed for their specificity and sensitivity using the colorimetric method.

3.3 Specificity and sensitivity of thiol modified aptamers

Three thiol modified aptamers (OO36F-SH, OO40F-SH and OO47F-SH) were assessed the specificity to distinguish DETP from other metabolites of organophosphates and pesticides using the colorimetric method. In all 3 aptamer reactions, the color of the AuNPs changed after the induction by NaCl following DETP detection, but it was not altered when paraquat and carbamate were investigated (Fig. 3, left). This suggested specific recognition of OO36F-SH, OO40F-SH and OO47F-SH for DETP but not for the other above-mentioned molecules. However, DEDTP which has a similar structure to DETP could induce AuNPs aggregation before NaCl was applied (data not shown), implying that the small molecule with a thiol group could autonomously drive the AuNPs to come together and increase the absorption at 650 nm of the AuNPs.

After the induction by NaCl following target application, only OO36F-SH had a ratio A₆₅₀/520 nm of the AuNPs in the presence of DETP that was statistically different from DEP, DMP, paraquat, carbamate and the control and was not lower than for DEDTP (right graph of Fig. 3). This experiment led to the conclusion that OO36F-SH coating on the AuNPs bound DETP more selectively than OO40F-SH and OO47F-SH did.

To evaluate the dissociation constant (K_d), DETP was added into the aptamer coated AuNPs in a dose-dependent manner, accompanied by NaCl aggregation induction. Color alterations of the AuNPs were observed by the naked eye (Fig. 4, top). Subsequently the values of the absorption ratio (A₆₅₀/A₅₂₀ nm) were measured and plotted against various DETP concentrations. The K_d values were analyzed using non-linear regression (curve fit) as demonstrated in Fig. 4. It was clear when observed with the naked eye that the AuNPs altered the color after 0.5 μM of DETP was added and detected by the AuNPs coated with OO36F-SH (Fig. 4a, top). However, there were inconclusive color changes in the reactions involving OO40F-SH and OO47F-SH (Fig. 4b and 4c, top). The dose-response curve revealed that the saturation of signal occurred when 5.0 μM of DETP was added to interact with the OO36F-AuNPs (Fig. 4a, bottom curve). With higher amounts of DETP, 10.0 μM was required to interact with OO40F-SH and OO47F-SH to reach saturation (Fig. 4b and 4c, bottom curve). The K_d analysis demonstrated that OO36F-SH had the highest affinity for DETP (0.103 ± 0.014 μM), while OO40F-SH and OO47F-SH had less affinity (K_d 0.388 ± 0.093 μM and 0.593 ± 0.046 μM, respectively). The R² value was greater than 0.9000 (suggesting a reliable curve fit) only for OO36F-SH and OO47F-SH (R² values of 0.9248 and 0.9651, respectively). This experiment indicated that OO36F-SH had the highest affinity to DETP, compared with the other aptamers,

and that it was suitable for using as the recognition unit in a colorimetric sensor to detect DETP at amounts greater than 0.5 μM by naked eyes.

3.4 Secondary structure

The sequences of 3 selected aptamers were used to predict the secondary structures based on RNAfold. The results revealed bulges and hairpin loops in all 3 aptamers (Fig. 5). Such secondary structures in the region of the 10–15 nucleotide length could hypothetically bind to a target (Zhou et al. 2010). The AC sequences in the hairpin loops of OO36F and OO40F likely contributed to the higher binding affinity than the AC-absent loop of the OO47F aptamer, which corresponded to their K_d values. The stability of the aptamer structure was also estimated and represented in free energy of the thermodynamic ensemble. Of the two aptamers having high binding to DETP, OO36F with free energy of -8.07 kcal/mol was more stable than OO40F with free energy of -9.33 kcal/mol.

This research unprecedentedly selected aptamers binding DETP, the metabolite of organophosphates, using CE-SELEX and a colorimetric aptasensor. Previous work used modified SELEX to screen ssDNA interacting with four organophosphates (Wang et al. 2012). Although it could select aptamers binding isocarbophos, omethoateas, phorate and profenofos simultaneously, it required 12 rounds of SELEX, immobilization of the ssDNA library and elution steps. Such challenging steps for conventional SELEX could prevent full interaction between the immobilized ssDNA and the target, and could remain the highest-affinity ssDNA in the column during elution step (Mendonça and Bowser 2004). These limitations could be overcome by performing CE-SELEX which did not require the immobilization and elution.

Recent studies have used synthesized ssDNA as binding units of pesticides or organophosphates, with AuNPs as the optical sensor. Acetamiprid at amounts higher than 2.5 mM could be visibly detected (Tian et al. 2016). Omethoate in the range 0.1–0.5 $\mu\text{g/ml}$ could also be investigated based on the same principle of the biosensor (Liu et al. 2020). The colorimetric aptasensors demonstrated the limit of detection for phorate at 10 μM (Bala et al. 2016) and for malathion at 1 pM (Bai et al. 2015).

The aptamer OO36F presented the lowest K_d at 0.1 μM and could apparently detect a minimum amount of DETP at 0.5 μM with the naked eye. However, none of our aptamers could work efficiently in the presence of DEDTP because it is a small molecule with a thiol group and hence could induce the aggregation of AuNPs before NaCl induction. Thus, the colorimetric assay to detect DETP is not specific when investigating the exposure for disulfoton, ethion, phorate or terbufos which are the parent compounds of both DETP and DEDTP. Hence, an application is still required that does not rely on the aggregation of AuNPs.

3.5 Electrochemical impedance spectroscopy

A thiol-modified aptamer was integrated with SPE to selectively detect DETP, DEDTP or DEP. The changes in R_{ct} were presented in a Nyquist plot (Fig. 6a). The R_{ct} on the surface of the aptamer coated with SPE increased when 0.025 $\mu\text{g/ml}$ of DETP, DEDTP or DEP was detected, compared with MCH blocking. The

percentage change in Rct was calculated using: $(Rct \text{ of target} - Rct \text{ of MCH}) / Rct \text{ of MCH} \times 100$ and the mean values are presented in Fig. 6b. The binding of DETP to the aptamer increased the Rct (\pm SD) to $47.5 \pm 8.8\%$ which was significantly higher than the altered Rct of DEDTP at $14.3 \pm 1.5\%$ and of DEP at $7.0 \pm 1.4\%$. The results demonstrated that EIS could be used to detect the altered Rct when DETP, DEDTP or DEP are bound to the OO36F aptamer that was immobilized on the gold surface.

The gold surface on the electrode was blocked by MCH after the thiol-modified OO36F aptamer was immobilized. This could overcome the simultaneous aggregation of AuNPs caused by DEDTP during colorimetric assay. The preliminary EIS results demonstrated that the OO36F aptamer could be used to detect the metabolites of organophosphates with higher selective binding to DETP than DEDTP and DEP.

A single concentration of the metabolites at $0.025 \mu\text{g/ml}$ was measured which equals to $0.148 \mu\text{M}$ of DETP and is close to the K_d value of OO36F to DETP, achieved from the colorimetric assay. Additionally Davies and colleagues used advanced GC technique and reported $0.09 \mu\text{g/ml}$ of DETP as the lowest amount found among urine samples of patients suffering from poisoning with organophosphates (Davies and Peterson 1997). The current measurement indicated the sensitivity of OO36F coupling with the EIS method that can efficiently be used to detect DETP in real samples.

Electrochemical biosensors have been used to detect an organophosphate, due to their sensitivity, specificity and reproducibility (Eissa and Zourob 2017; Jiao et al. 2017; Xu et al. 2018). However, the current work unprecedentedly emphasized using aptasensors to detect the metabolite DETP, as this could provide the history of exposure of organophosphates that could be detoxified and transformed into dialkyl phosphates (Sudakin and Stone 2011). Furthermore, various concentrations of DETP measured using electrochemical sensing should be considered to investigate the limit of detection of the aptasensor. The additional investigation should use this aptasensor to measure DETP in fruit and vegetables that are spiked with organophosphates and kept at 4°C .

4. Conclusion

Aptamers specifically binding to DETP, a metabolite of organophosphates, were successfully generated using CE-SELEX. The selection of the highest-affinity aptamer to DETP was performed by observing the color change of AuNPs. OO36F had the lowest K_d of $0.103 \pm 0.014 \mu\text{M}$ with a clear color change of the AuNPs being observed with the naked eye at $0.5 \mu\text{M}$. The aptamer also selectively bound to DETP rather other organophosphate metabolites such as DEP and DMP. However, the colorimetric sensor using AuNPs coated with OO36F was not suitable for the detection of DEDTP which is another metabolite of the same parent compound as DETP.

The thiol-modified OO36F aptamer was then used to fabricate an aptamer-based electrochemical sensor. The aptamer-immobilized gold electrode detected the change of Rct when the aptamer was bound to the targets on the gold surface that blocked non-specific binding by any thiol processing molecules, especially DEDTP. It could detect DETP at $0.025 \mu\text{g/ml}$ or $0.148 \mu\text{M}$ and had a significantly higher Rct value than either DEDTP or DEP at the same concentration. These results indicated the great potential to

use the aptasensor to indicate the history of exposure of organophosphates by detecting trace amounts of the metabolite DETP, although biodegradation of organophosphates in samples might occur.

Declarations

Acknowledgement

The author would like to thank Kasetsart University Research & Development Institute (KURDI) for language editing service.

Funding

This study is supported by National Research Council of Thailand, Kasetsart University Research and Development Institute, (grant no. KURDI (FF(KU)6.64)), and the Omics Center for Agriculture, Bioresources, Food and Health, Kasetsart University (OmiKU)

Conflicts of interest

The authors declare that they have no conflict of interest.

References

Bai W, Zhu C, Liu J, Yan M, Yang S, Chen A (2015) Gold nanoparticle-based colorimetric aptasensor for rapid detection of six organophosphorous pesticides *Environ Toxicol Chem* 34:2244-2249 doi:10.1002/etc.3088

Bala R, Sharma RK, Wangoo N (2016) Development of gold nanoparticles-based aptasensor for the colorimetric detection of organophosphorus pesticide phorate *Anal Bioanal Chem* 408:333-338 doi:10.1007/s00216-015-9085-4

Davies JE, Peterson JC (1997) Surveillance of occupational, accidental, and incidental exposure to organophosphate pesticides using urine alkyl phosphate and phenolic metabolite measurements *Ann N Y Acad Sci* 837:257-268 doi:10.1111/j.1749-6632.1997.tb56879.x

Eissa S, Zourob M (2017) Selection and Characterization of DNA Aptamers for Electrochemical Biosensing of Carbendazim *Anal Chem* 89:3138-3145 doi:10.1021/acs.analchem.6b04914

Jiao Y, Hou W, Fu J, Guo Y, Sun X, Wang X, Zhao J (2017) A nanostructured electrochemical aptasensor for highly sensitive detection of chlorpyrifos *Sensors and Actuators B: Chemical* 243:1164-1170 doi:<https://doi.org/10.1016/j.snb.2016.12.106>

Kongtip P et al. (2017) The Impact of Prenatal Organophosphate Pesticide Exposures on Thai Infant Neurodevelopment *Int J Environ Res Public Health* 14 doi:10.3390/ijerph14060570

Liu DL, Li Y, Sun R, Xu JY, Chen Y, Sun CY (2020) Colorimetric Detection of Organophosphorus Pesticides Based on the Broad-Spectrum Aptamer J Nanosci Nanotechnol 20:2114-2121 doi:10.1166/jnn.2020.17358

Lu C, Bravo R, Caltabiano LM, Irish RM, Weerasekera G, Barr DB (2005) The presence of dialkylphosphates in fresh fruit juices: implication for organophosphorus pesticide exposure and risk assessments J Toxicol Environ Health A 68:209-227 doi:10.1080/15287390590890554

Mendonsa SD, Bowser MT (2004) In vitro evolution of functional DNA using capillary electrophoresis J Am Chem Soc 126:20-21 doi:10.1021/ja037832s

Ohshiro K, Kakuta T, Sakai T, Hirota H, Hoshino T, Uchiyama T (1996) Biodegradation of organophosphorus insecticides by bacteria isolated from turf green soil Journal of Fermentation and Bioengineering 82:299-305 doi:[https://doi.org/10.1016/0922-338X\(96\)88823-4](https://doi.org/10.1016/0922-338X(96)88823-4)

Racke K 3@ Degradation of Organophosphorus Insecticides in Environmental Matrices. In, 1992.

Simaremare SRS, Hung CC, Hsieh CJ, Yiin LM (2019) Relationship between Organophosphate and Pyrethroid Insecticides in Blood and Their Metabolites in Urine: A Pilot Study Int J Environ Res Public Health 17 doi:10.3390/ijerph17010034

Sudakin DL, Stone DL (2011) Dialkyl phosphates as biomarkers of organophosphates: the current divide between epidemiology and clinical toxicology Clin Toxicol (Phila) 49:771-781 doi:10.3109/15563650.2011.624101

Tian Y, Wang Y, Sheng Z, Li T, Li X (2016) A colorimetric detection method of pesticide acetamiprid by fine-tuning aptamer length Anal Biochem 513:87-92 doi:10.1016/j.ab.2016.09.004

Wang L, Liu X, Zhang Q, Zhang C, Liu Y, Tu K, Tu J (2012) Selection of DNA aptamers that bind to four organophosphorus pesticides Biotechnol Lett 34:869-874 doi:10.1007/s10529-012-0850-6

Xu G, Huo D, Hou C, Zhao Y, Bao J, Yang M, Fa H (2018) A regenerative and selective electrochemical aptasensor based on copper oxide nanoflowers-single walled carbon nanotubes nanocomposite for chlorpyrifos detection Talanta 178:1046-1052 doi:10.1016/j.talanta.2017.08.086

Zhang X, Driver JH, Li Y, Ross JH, Krieger RI (2008) Dialkylphosphates (DAPs) in fruits and vegetables may confound biomonitoring in organophosphorus insecticide exposure and risk assessment J Agric Food Chem 56:10638-10645 doi:10.1021/jf8018084

Zhou J, Battig MR, Wang Y (2010) Aptamer-based molecular recognition for biosensor development Anal Bioanal Chem 398:2471-2480 doi:10.1007/s00216-010-3987-y

Figures

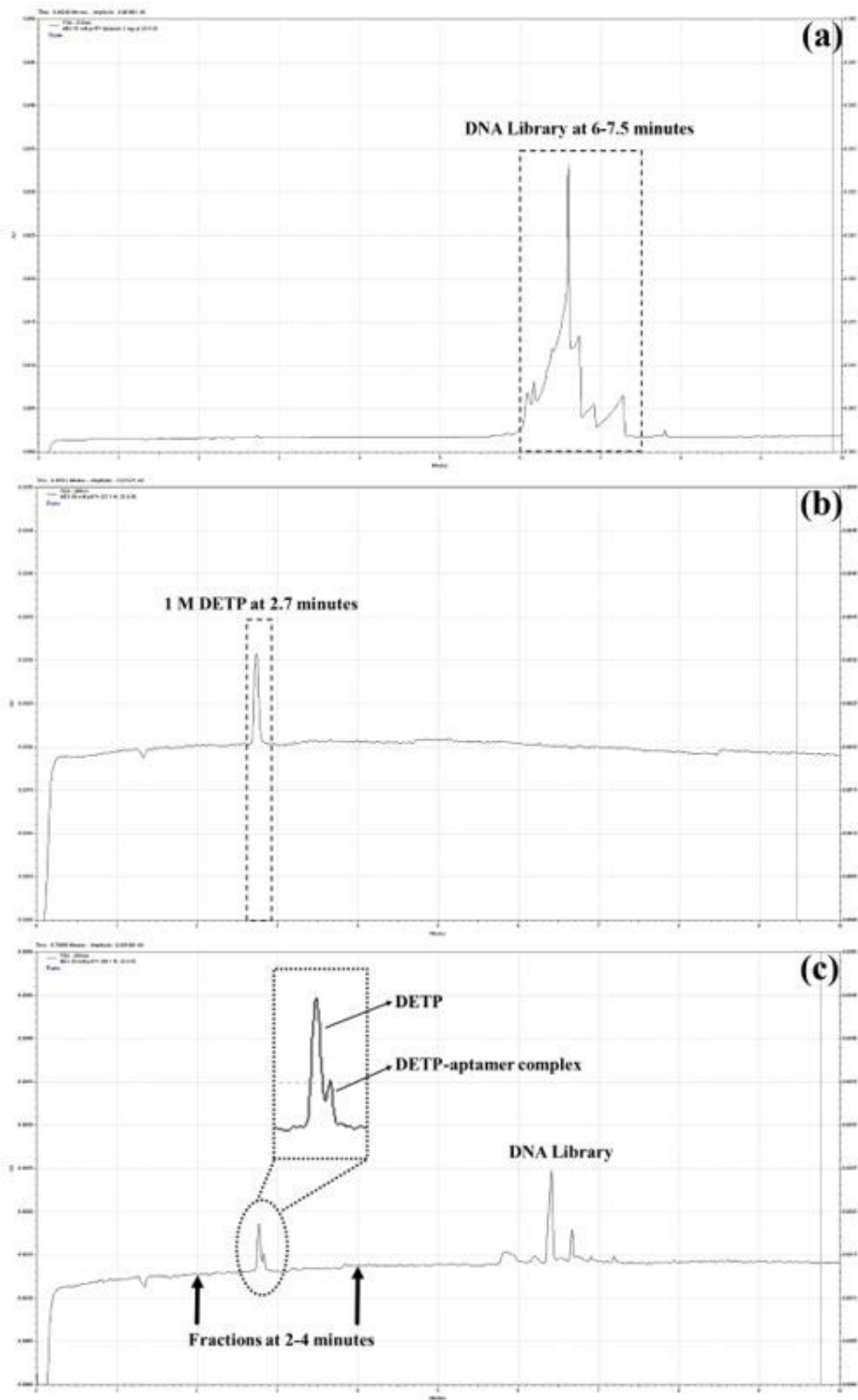


Figure 1

Electropherogram of CE-SELEX selection Capillary electropherogram of (a) ssDNA library, (b) 1 M DETP and (c) free-DETP, DETP-aptamer complex and separated unbound ssDNA library.

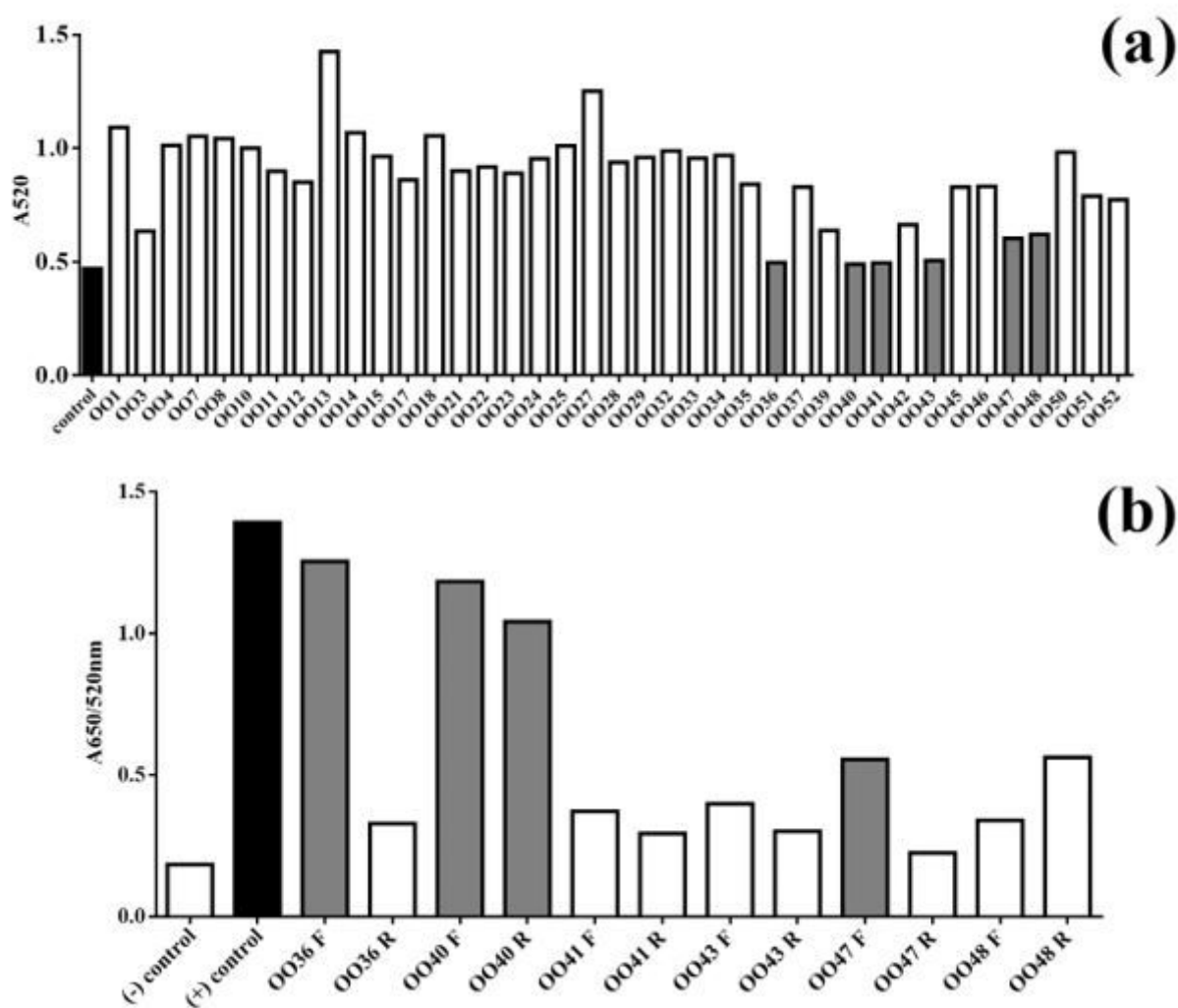


Figure 2

Colorimetric screening for aptamer candidates (a) denatured PCR product. Graph of absorption at 520 nm by the AuNPs was plotted against 250 ng of 39 denatured PCR products. The remaining red-wine particles (A_{520nm}) were observed after adding 100 μM DETP and 2 N NaCl, compared with the red particles left in the control without any presence of ssDNA. (b) asymmetric-PCR-product ssDNA. Forward and reverse strands of 6 PCR products were generated using asymmetric PCR. Changes in gold aggregation were observed after allowing forward or reverse ssDNA on the AuNPs to bind DETP and being induced by 2 N NaCl. The absorption ratio was compared with the possible maximum ratio of the positive control reaction consisting of AuNPs and 2 N NaCl and negative control which contained only the AuNPs without inducing aggregation by NaCl.

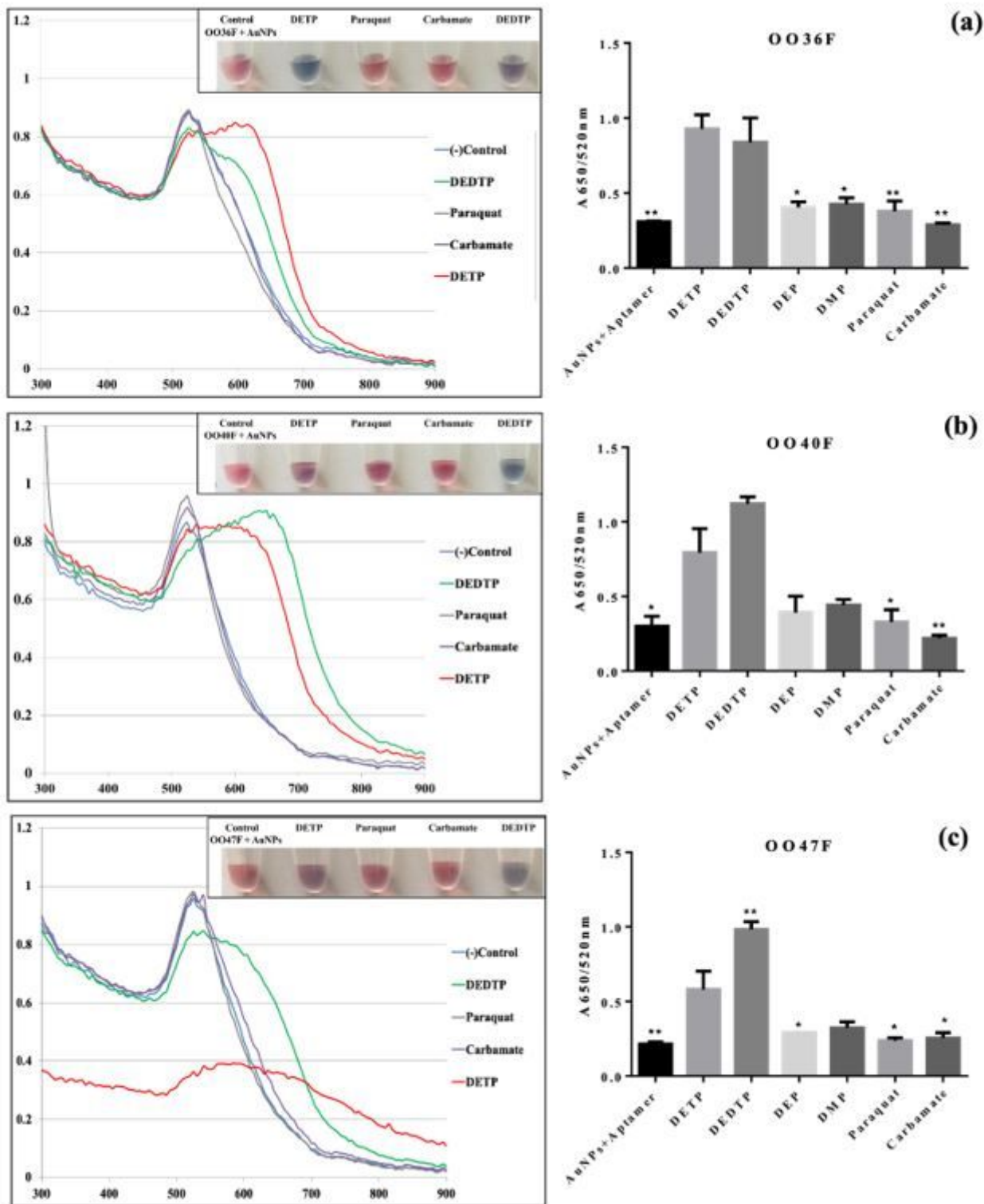


Figure 3

Specificity of selected thiol-modified aptamers Plot of absorption spectrum (left) with the corresponding color changes of AuNPs (inset) and a graph of A_{650/520nm} ratio of the AuNPs (right) of (a) OO36F-SH, (b) OO40F-SH and (c) OO47F-SH. The absorption ratio of AuNPs was demonstrated after 0.5 μM of aptamers was mixed with AuNPs and 100 μM of DETP, DEDTP, DEP, DMP, paraquat or carbamate, followed by 2 N NaCl induction. The reaction without any targets of each aptamer was included as the

negative control. The mean absorption ratio ($n = 2-3$), of every chemical was plotted and compared with the mean value of DETP using the Graphpad Prism 6 software. The statistically significant results were presented at $p < 0.5$ (*) and $p < 0.01$ (**).

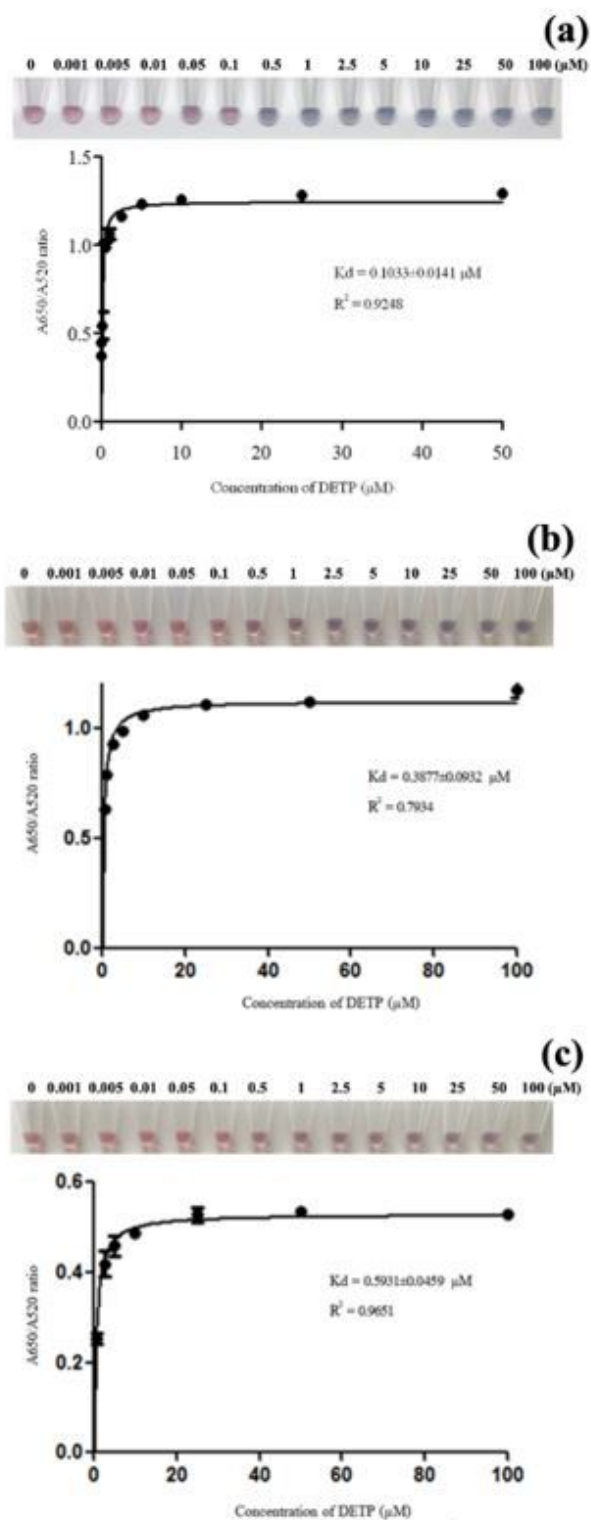


Figure 4

Sensitivity of selected thiol-modified aptamers for DETP Non-linear regression curve of (a) 0036F-SH, (b) 0040F-SH and (c) 0047F-SH with color changes of AuNPs (inset). Concentrations of DETP (0, 0.001,

0.005, 0.01, 0.05, 0.1, 0.5, 1, 2.5, 5, 10, 25, 50 and 100 μM) are represented on x-axis in all figures. Y-axis is the absorption ratio of 650 to 520 nm of AuNPs. All three aptamers were used to coat the AuNPs at 0.5 μM followed by mixing with DETP and inducing by 2N NaCl. The mean of the absorption ratio (A_{650}/A_{520} , $n = 3$) was used to enumerate the dissociation constant (K_d) of each aptamer to DETP based on GraphPad Prism 6, Nonlinear Regression (curve fit).

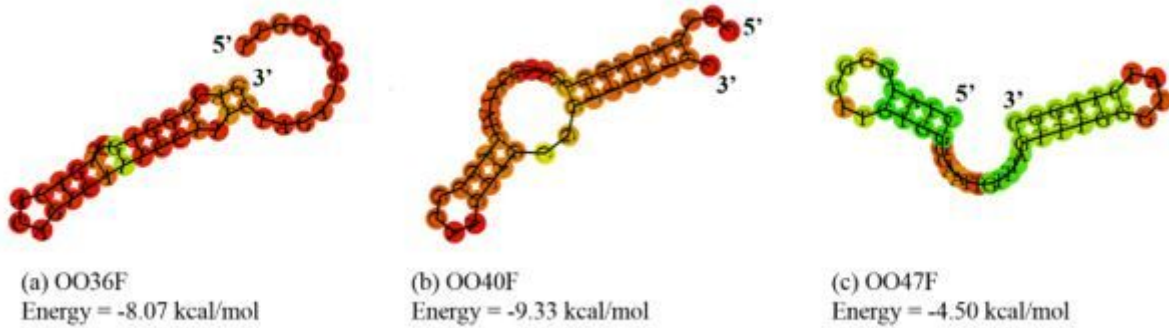


Figure 5

Secondary structure and sequences of strong aptamer candidates Nucleotide sequences of (a) OO36F, (b) OO40F and (c) OO47F aptamers were predicted for their secondary structure and free energy based on RNAfold program. Blue, green, yellow, brown and red colors depict probability of base-pairing from 0 to 1, respectively.

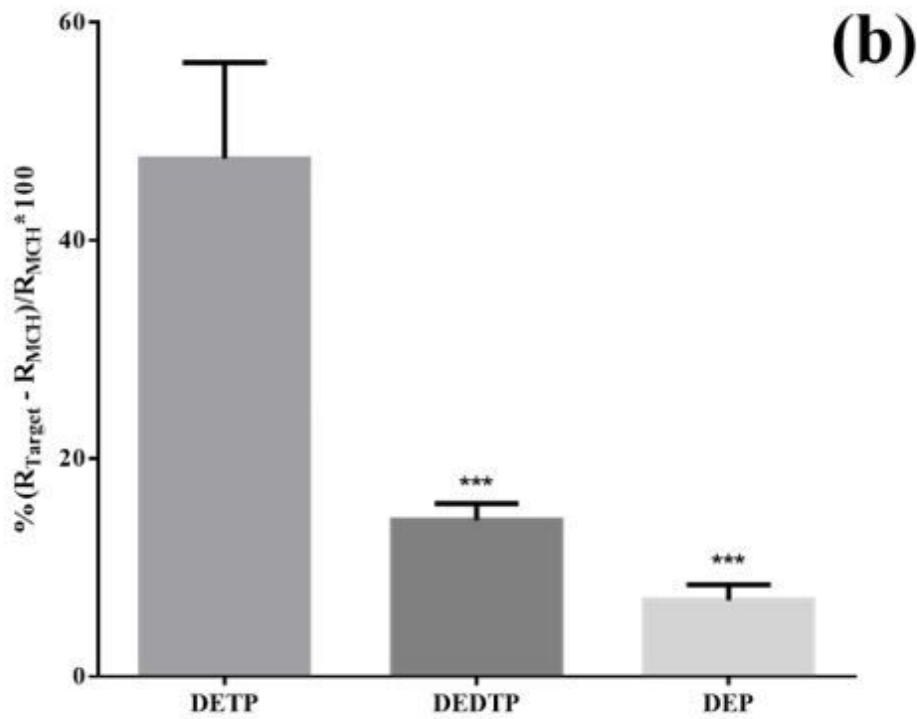
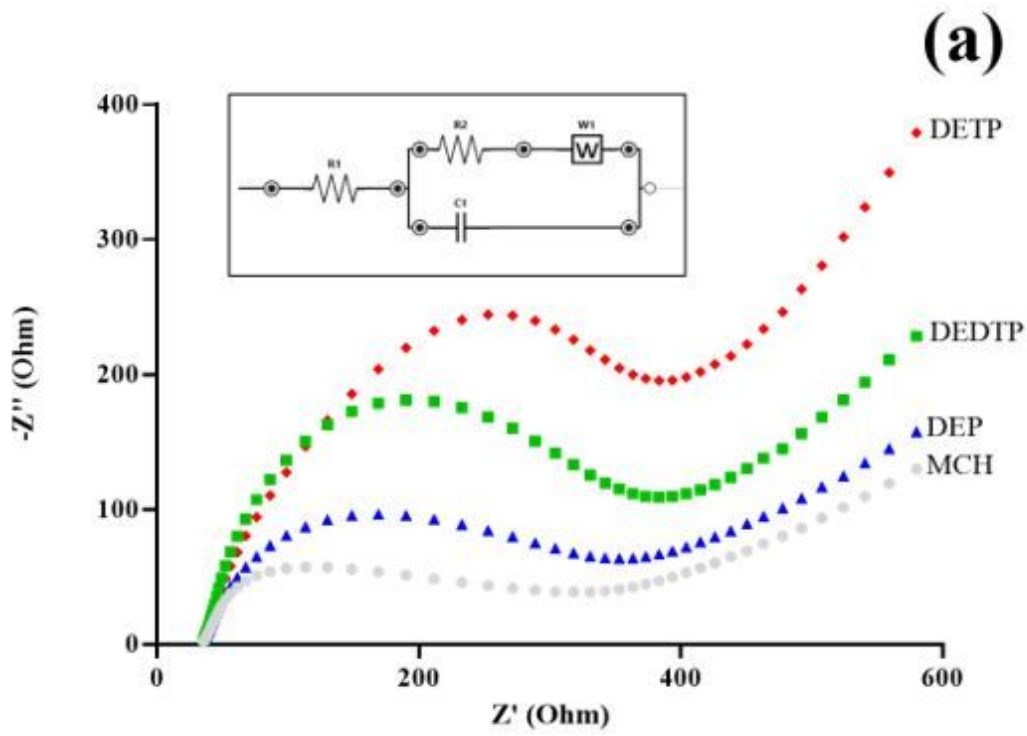


Figure 6

EIS responses of DETP, DEDTP and DEP Nyquist plots (a) on responses of 0.025 $\mu\text{g/ml}$ of DETP (red diamond), DEDTP (green square) and DEP (blue triangle) and aptamer-coated electrodes which were blocked with MCH (grey circle). Modified Randles equivalent circuit was used to fit the impedance spectra and is presented in the inset. Comparative aptasensor response (b) presented as percentages of altered Rct of DETP, DEDTP and DEP. The average of 3 individual experiments is presented in the bar graph and

error bars indicate SD. The percentage of altered Rct was analyzed using one-way ANOVA with significant difference from DETP at $p < 0.001$ (***)).